Available online at www.sciencedirect.com

SCIENCE DIRECT®

Geomorphology 67 (2005) 317–334

GEOMORPHOLOGY

www.elsevier.com/locate/geomorph

Selective glacial erosion and weathering zones in the coastal mountains of Marie Byrd Land, Antarctica

David E. Sugden[a,*], Greg Balco[b], Seth G. Cowdery[b], John O. Stone[b], Louis C. Sass III[c]

[a]*Institute of Geography, School of GeoSciences, University of Edinburgh, Drummond Street, Edinburgh, Scotland, EH8 9XP, UK*
[b]*Quaternary Research Center and Department of Earth and Space Sciences, Box 351360, Seattle, WA 98195-1360, USA*
[c]*Geology Department, Colorado College, Colorado Springs, CO 80903, USA*

Received 12 January 2004; received in revised form 13 October 2004; accepted 14 October 2004
Available online 16 December 2004

Abstract

In the coastal mountains of Marie Byrd Land, Antarctica, there is a juxtaposition of ice moulded landforms at lower altitudes and upstanding summits with weathered surfaces bearing tors. This paper uses geomorphological mapping and exposure dating to test two hypotheses commonly used to explain such a landscape contrast: either the pattern reflects contrasts in glacial erosion related to the basal thermal regime beneath a former ice sheet or it represents a periglacial trimline marking the upper limit of ice cover during the Last Glacial Maximum (LGM). Cosmogenic nuclide measurements on erratics show that the mountains were covered by ice on several occasions, most recently during the LGM. Similar measurements on bedrock show that fragile landforms on weathered surfaces survived many glaciations. Nuclide concentrations in bedrock indicate both that subglacial erosion is insignificant and that ice-free periods of periglacial weathering are longer at higher elevations. We conclude that the pattern of landscape modification reflects both topographically controlled contrasts in the basal thermal regime of overriding ice and the longer exposure to periglacial conditions at higher elevations. In addition, the combination of nuclide data and the wider pattern of striations shows that the LGM ice cover was thinner than predicted by ice sheet models assuming equilibrium conditions, that ice sheet thinning has occurred from 10,400 years ago to the present, and that regional flow by overriding ice has been replaced by radial ice flow from local glaciers centred on individual mountain massifs.
© 2004 Elsevier B.V. All rights reserved.

Keywords: West Antarctic Ice Sheet; Marie Byrd Land; Glacial geomorphology; Glaciology; Cosmogenic isotopes; Weathering zones

1. Introduction

In this paper, we describe and analyse the glacially modified landscape of the Ford Ranges, which rise above the ice sheet surface in the peripheral zone of part of the West Antarctic Ice

* Corresponding author. Tel.: +44 131 6507543; fax: +44 131 6502624.
E-mail address: David.Sugden@ed.ac.uk (D.E. Sugden).

0169-555X/$ - see front matter © 2004 Elsevier B.V. All rights reserved.
doi:10.1016/j.geomorph.2004.10.007

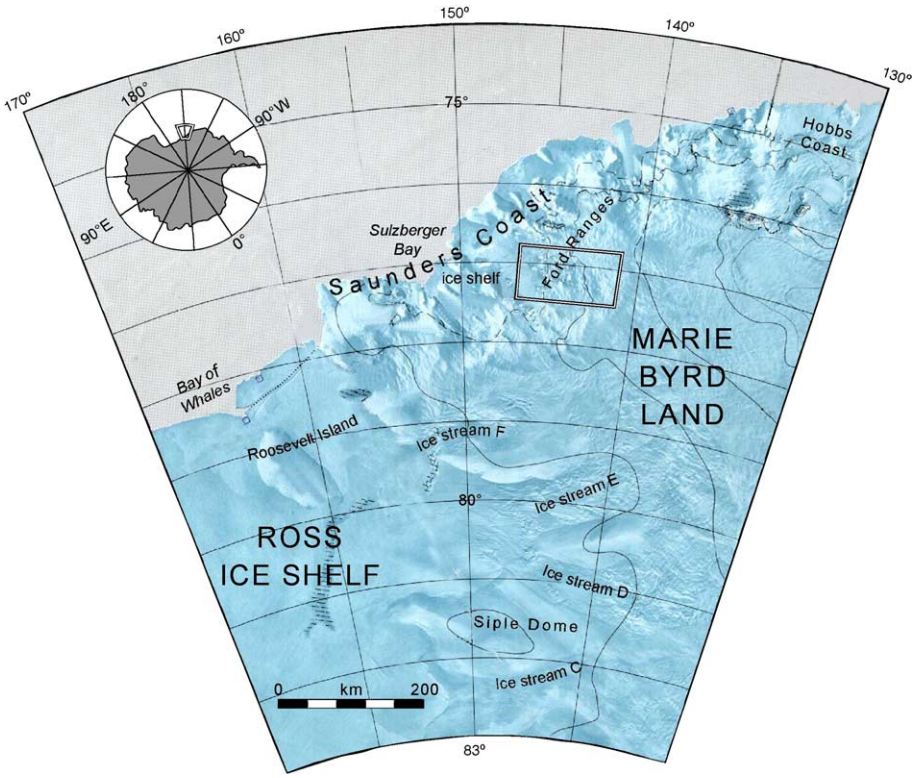

Fig. 1. Location of the Ford Ranges in Marie Byrd Land and their relationship to the Ross Ice Shelf and Ice Streams E and F. After Satellite Image Map of Antarctica, U.S. Geological Survey, 1996. Inset shows the location of Fig. 3.

Sheet in Marie Byrd Land (Fig. 1). Our aim is to distinguish between competing explanations for the contrast between strongly weathered summits and ice-moulded terrain at lower elevations. This contrast is particularly clear in the Sarnoff and Allegheny Mountains. On many of these mountains, there is a juxtaposition of strongly moulded landforms of glacial erosion at lower altitudes and upstanding summits with weathered surfaces, tors and granular granite grus (Fig. 2).

Fig. 2. The massif of Mount Rea, Sarnoff Mountains, Marie Byrd Land, showing the rolling upper surface on which there are tors. Ice-moulded slopes occur at lower altitudes on the massif flanks. The mountains overlook outlet glaciers flowing towards the coast.

Two hypotheses are commonly invoked to explain such a landscape contrast. One is that the juxtaposition is the result of a modification beneath an overriding ice sheet; low-altitude surfaces are eroded by sliding, warm-based ice, while higher summits are protected by thinner, cold-based ice. This has been argued for landscapes in Scotland (Sugden, 1968), Scandinavia (Kleman and Stroeven, 1997; Stroeven et al., 2002; Fabel et al., 2002) and Arctic Canada (Sugden and Watts, 1977; Sugden, 1978; Bierman et al., 1999; Briner et al., 2003). From the range of variables affecting basal thermal regime, two critical factors at the scale of individual mountain massifs are, first, the contrast in ice thickness between the summits and intervening lowland and, second, the presence of diverging ice over summits and the converging ice over lowlands, leading to contrasts in ice velocity. Both factors favour colder ice over uplands and warmer ice over lowlands, with the latter factor being the most important on the scale of mountains and valleys (Glasser, 1995). The protective role of cold-based ice has been questioned on theoretical grounds by Shreve (1984) and on the basis of field observations beneath Meserve Glacier in the McMurdo Dry Valleys (Cuffey et al., 2000). Furthermore, there is growing evidence that cold-based ice can erode fine striations and transport basal debris under certain conditions (Atkins et al., 2002). As stimulating as the latter ideas are, there is, as yet, no firm evidence that cold-based ice can erode sufficiently to transform a landscape and create significant landforms of glacial erosion.

A powerful alternative hypothesis to explain the contrast between glacially eroded landforms at low altitudes and unmodified summits is that the latter simply escaped glaciation. When faced with the existence of tors in Britain and Scandinavia, Linton (1949, p. 32) wrote “they can hardly have survived the passage across them of even the feeblest stream of moving ice”. His concept of unglaciated enclaves was applied widely and is still current in areas of Buchan in Northeast Scotland. Subsequently, it has been reinforced by the idea that the boundary between landscape types may represent a former glacial trimline. Whereas the ice scoured the landforms below the margin, the upstanding summits represent nunataks that rose above the former ice surface, where they were exposed to weathering under periglacial conditions. There have been several ice sheet reconstructions based on such observations, e.g., in northern Victoria Land (Orombelli et al., 1990), the Canadian Arctic (Boyer and Pheasant, 1974), Scandinavia (Nesje and Sjerup, 1988; Nesje, 1989) and Scotland (Ballantyne, 1990; McCarroll et al., 1995; Ballantyne et al., 1998). Such reconstructions of former ice sheets are significant because they provide field constraints on former ice thickness, a critical factor when modelling ice sheet behaviour.

Thus, it is important for our understanding of the West Antarctic Ice Sheet to establish whether marginal mountains were submerged beneath overriding ice or whether they survived the Last Glacial Maximum (LGM) as nunataks. In an effort to answer this question, we report geomorphic analyses, as well as cosmogenic-nuclide measurements, on glacial erratics and bedrock surfaces in the Sarnoff and Allegheny Mountains.

2. Setting

The Sarnoff and Allegheny Mountains comprise a WNW–ESE oriented chain within the Ford Ranges of Marie Byrd Land (Fig. 1). The summits are 700–1100 m above sea level and overlook glaciers flowing to the Sulzberger Ice Shelf on the Saunders Coast. Arthur Glacier, to the immediate north, has a local mountain catchment, while the 12-km-wide Boyd Glacier and the even larger Hammond Glacier, further to the south, drain the ice sheet dome inland of the Ford Ranges (Fig. 3). The inland flanks of this latter dome are drained by Ice Streams E and F, discharging to the Ross Ice Shelf (Fig. 1). The concentration of transverse crevassing without a significant change in elevation in the vicinity of Mt. Blades and Bailey Ridge suggests that this may mark the grounding line of the Boyd Glacier.

The broad shape of the subglacial topography is shown in Fig. 4. The Ford Ranges represent the highest ground, while the bedrock underlying the inland dome is an arcuate area of ground above sea level, separating the outer coast from the Siple Coast of the Ross Sea embayment. The outer coast itself consists of a broad offshore shelf, dotted with

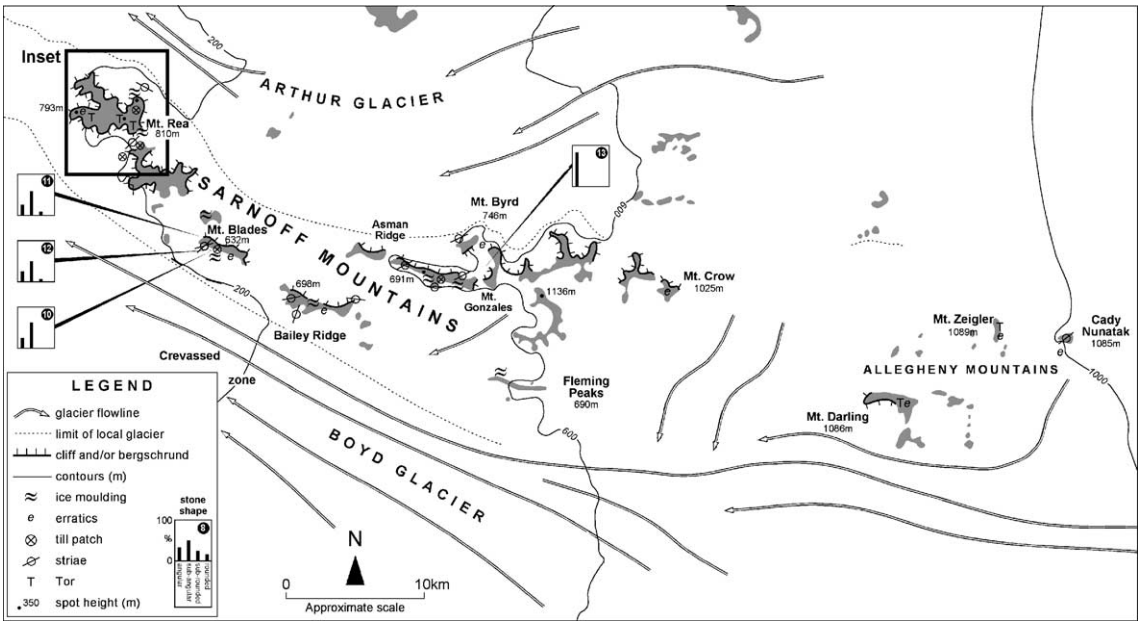

Fig. 3. The Sarnoff and Allegheny mountains (shaded) showing the Boyd and Arthur glaciers, limits of local ice centred on the Sarnoff massif, features of glacial erosion, erratics, till patches and stone shape characteristics. Inset shows the location of Fig. 5.

upstanding islands covered by ice domes and linked by the Sulzberger Ice Shelf. The abrupt edge of the continental shelf is some 160 km distant from the western end of the Sarnoff Mountains.

3. Approach

The geomorphology of upstanding mountains was examined and mapped at two scales. In areas of little bedrock exposure, features were examined in the field and mapped at a scale of 1:250,000 (Fig. 3). In the area of greater exposure in the vicinity of Mt. Rea, a geomorphological map was created using vertical air photographs, backed up by field observations (Fig. 5). Altitudes were obtained using barometers calibrated to a series of control points obtained by differential GPS surveying.

We collected samples from glacially transported erratics, as well as bedrock surfaces for cosmogenic-nuclide analysis. The bedrock samples were from windswept surfaces free of soil or sediment, where snow accumulation would be unlikely. Where possible, we collected erratics from bedrock surfaces to avoid the possibility of displacement by periglacial processes. At higher elevation, we collected erratics resting on, or slightly embedded in, thin patches of regolith. Details of sampling and analytical methods appear in Stone et al. (2003a,b). The methods used to calculate exposure ages from nuclide concentrations also appear in Stone et al. (2003b).

4. Geomorphology

The glacial geomorphology reflects two assemblages of landforms: features associated with present day local glaciers and features associated with overriding ice that covered all the mountains in the past.

4.1. Local glaciation

Local glaciers are centred on the upstanding mountain massifs and flow approximately radially towards the bounding outlet glaciers. The boundary between local ice and the outlet glaciers is sharp and reproduced in Fig. 3. Radially outward flow from the mountains and ridges is demonstrated by bergschrunds at the head of the local glaciers. There is marked asymmetry across transverse ridges, such as

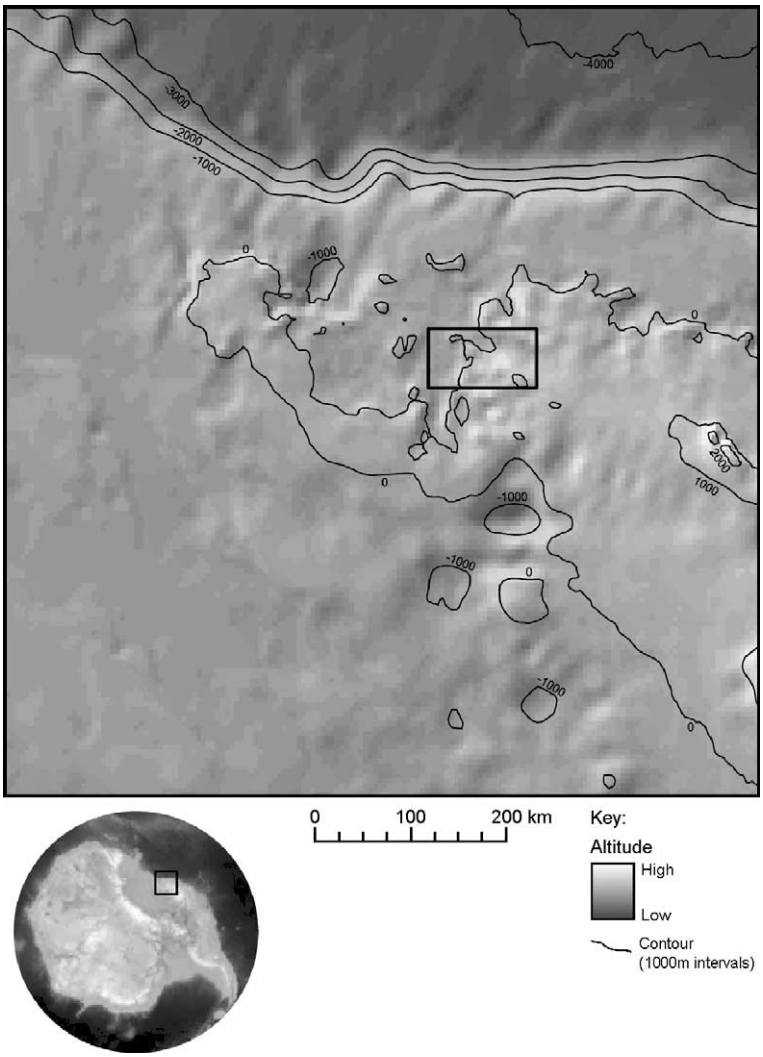

Fig. 4. Subglacial morphology of the wider region. Hill shaded DEM from BEDMAP (5 km). (www.antarctica.ac.uk/aedc/bedmap/). Inset shows the location of Fig. 3.

the Bailey and Asman Ridges. On the upwind northern side, the ridge flanks are exposed, and cliffs and/or rectilinear bedrock slopes may rise several hundred meters above the glacier surface. In places, there may be a windscoop exposing blue ice. On the lee southern side, drifts of snow and ice commonly extend from within metres of the ridge crest down to the glacier below. Some lee-side drifts may be several kilometres in length.

Although the local glaciers are cold based, they are agents of geomorphological denudation. Evidence of erosion comes from the association of bergschrunds with backing rock cliffs. In places such as around Mt. Dolber, precipitous cliffs have discharged rockfall debris onto glaciers at their foot. Elsewhere, such as on Bailey and Asman ridges, a rectilinear slope of 30° may be oversteepened in its lower reaches in the vicinity of the bergschrund. The transport of rock material is well illustrated in the case of glaciers on the south and western sides of Mt. Rea (Fig. 5). Here, there are surface moraines extending away from the cliffs before they eventually become absorbed downstream in the continuing accumulation zone of the glacier.

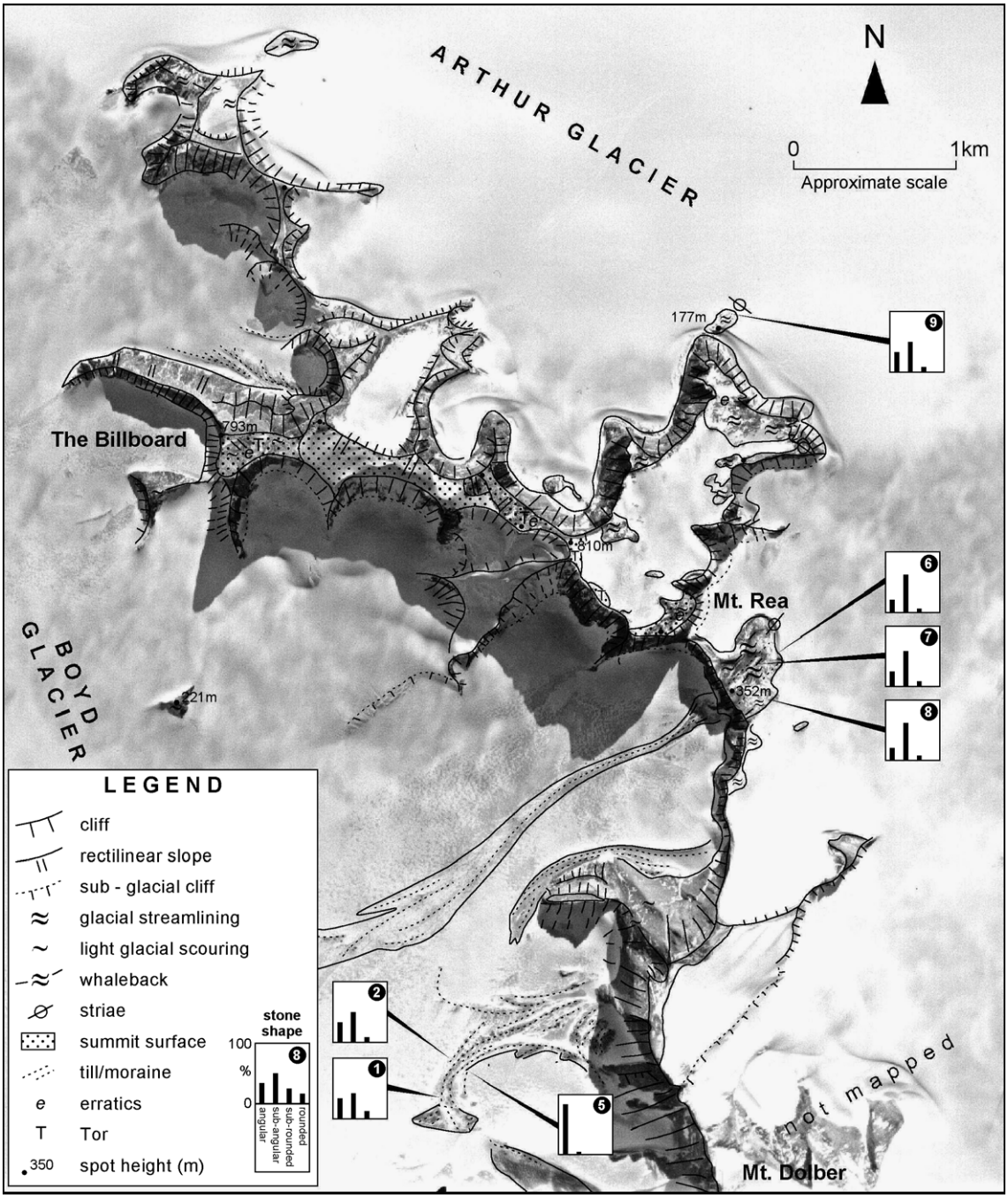

Fig. 5. Geomorphological map superimposed on vertical air photographs of Mt. Rea, The Billboard and the flanks of Mt. Dolber. Stone roundness details are also shown.

In two places, there are loop moraines bounding local corrie glaciers, namely, on the western flanks of Mt. Gonzalez and Mt. Dolber. In both cases, the local glacier ends in a blue-ice ablation zone and debris accumulates on the ice sheet surface rather than being transported away. The material in the local moraines is angular, devoid of a fine matrix and consists wholly of local lithologies. Thus, the Gonzalez moraine consists only of local granite, while the innermost Dolber moraine consists of the granites and metasediments exposed in the cliffs behind (Table 1). No basal ice exposures were seen associated with either local moraine. Indeed, the ice immediately below the Gonzalez moraine ridge consisted of steeply dipping, foliated, debris-free ice with flattened air bubbles. Such characteristics in the terminal zone of deposition are typical of cold-based glaciers whose geomorphological role is restricted to the transport of surface-derived rockfall material.

4.2. Past overriding by ice

The most obvious evidence of overriding ice includes erratic cobbles and boulders that occur on all mountains and ridges rising above the present ice surface (Fig. 6). The erratics comprise a variety of granites and metasediment boulders, with rare volcanics. Their exotic nature is demonstrated by the presence of metasediments on granite bedrock, as in the case of Mt Crow, or granites on ridges of metasediment, such as on Bailey Ridge. With the exception of Mt. McClung (1146 m) and its subsidiary peaks, erratics occur on or near the summits of many mountains and ridges in the Sarnoff and Allegheny

Table 1
Details of selected till deposits

No.	Location	Lat. S./Long. W.	Alt. (m)	Site	Lithology	Shape %				% Granite	% Striated (total)[a]
						A	SA	SR	R		
1	Mt. Dolber W.	77° 06 0.719	~115	Outermost ice-cored	Granite	34	30	4	0	68	8
		145° 37 0.346′		moraine ridge	metasediment	4	20	8	0		
2	Mt. Dolber W.	" "	~115	Outermost of 4 corrie	Granite	32	26	0	0	58	10
	(transect)			moraine ridge	metasediment	6	32	4	0		
3	Mt. Dolber W.	" "	~115	Third of four corrie	Granite	100	0	0	0	100	0
	(Transect)			moraine ridge	metasediment	0	0	0	0		
4	Mt. Dolber W.	" "	~115	Second of four corrie	Granite	34	16	0	0	50	0
	(Transect)			moraine ridge	metasediment	6	38	6	0		
5	Mt. Dolber W.	" "	~115	Innermost of four corrie	Granite	68	2	0	0	70	0
	(Transect)			moraine ridge	metasediment	30	0	0	0		
6	Rea-Dolber	77° 04 0.913′	~206	Loose till layer 2 m	Granite	22	16	2	0	40	6
	Saddle	145° 32 0.549′		from the ice edge	metasediment	2	56	2	0		
7	Rea-Dolber	77° 04 0.865′	~293	Sample from streamlined	Granite	24	30	2	0	56	2
	Saddle	145° 33 0.112′		till deposit	metasediment	6	36	2	0		
8	Rea-Dolber	77° 04 0.865′	~340	Till patch in hollow near	Granite	18	44	2	0	64	0
	Saddle	145° 33 0.272′		saddle crest	metasediment	2	28	6	0		
9	Mt. Rae	77° 03 0.615′	149	Till patch on	Granite	38	32	2	0	72	6
	(North Spur)	145° 34 0.215′		ice-moulded spur	metasediment	2	22	4	0		
10	Mt. Blades	77° 09 0.794′	472	Till patches on saddle	Granite	14	40	0	0	54	8
		145° 18 0.449′			metasediment	12	34	0	0		
11	Mt. Blades	77° 09 0.647′	608	Till in gully near west	Granite	28	32	2	0	62	0
		145° 19 0.595′		summit	metasediment	0	34	4	0		
12	Mt. Blades	77° 09 0.724′	419	Till sheet north side	Granite	22	24	6	0	52	2
		145° 18 0.175′		of saddle	metasediment	8	36	4	0		
13	M. Gonzalez	77° 10 0.813′	~536	Outer corrie glacier	Granite	100	0	0	0	100	0
		144° 34 0.514′		moraine	metasediment	0	0	0	0		

Information about lithology, clast shape and % of striated clasts is based on random counts of 50 stones after Reichelt (1961). Location of scale numbers are shown on Figs. 3 and 5.

[a] All striated stones were metasediments.

Fig. 6. Glacially streamlined whaleback landforms on the saddle between Mt. Rea and Mt. Dolber. An erratic boulder, approximately 1 m in diameter, is in the midforeground.

Mountains. This includes Cady Nunatak (1085 m) and Mt. Darling (1086 m) towards the inland ice dome and Mt. Blades (632 m), The Billboard (793 m) and Mt. Rea (810 m) towards the coast. The density of erratics decreases with altitude. Thus, on the higher summits of narrower ridges, there may be only one or two erratics in a 100 m^2 area, while at lower altitudes, there may be a more or less continuous scatter of boulders, or even a patch of till.

Details of the till patches visited are contained in Table 1. Patches occur in saddles, bedrock depressions and gullies at altitudes of up to 608 m near the western summit of Mt. Blades. Excluding local glacier tills, there is a mixture of granite and metasediment clasts with the proportion of granite ranging from 40% to 70%. Stone shape analyses demonstrate that 16–56% of clasts are subangular and are similar in percentage to the number of angular clasts in any sample. Commonly, 2–8% of clasts are subrounded. In many cases 2–10% of the clasts are striated; invariably, the latter are metasediments. The matrix is often gritty but has a fine component containing clay-sized particles. Till is particularly extensive on ice-moulded bedrock surfaces above the head of the glacier that flows from the northeastern side of the saddle between Mts. Rea and Dolber (Fig. 7). Close to the ice edge, it forms an unconsolidated layer 1–10 cm thick on all rock surfaces up to 16–22°. Further above the ice edge, the till is progressively confined to bedrock hollows.

Erosional forms also testify to the passage of overriding ice. Streamlined whaleback forms 75–100 m long, 20–25 m across, with a relief of 2–10 m, are orientated NE–SW in the saddle between Mts. Rea and Dolber (Fig. 6). Others occur around the flanks of Mt. Rea and in saddles on Bailey Ridge and Mt. Blades. Many ridges display roche moutonnée forms with convex northwestern slopes and oversteepened southwestern slopes. In many such locations, there are striations, gouges and crescentic cracks, the alignment of which conforms to that of the larger erosional forms. Striated surfaces occur on the top of Asman and Bailey ridges, Mts. Blades and Byrd, and Cady Nunatak. The orientation of the striae is towards the west and southwest, as demonstrated in Fig. 3. The mean true orientation is 263° in the Sarnoff Mountains and 230° on Cady Nunatak. Orientations diverge around Mt. Rea and range from 220° to 293°.

There is a marked altitudinal zonation in the way the landscape has been modified by ice. Landforms of glacial erosion are clearly developed at low altitudes. There is an intermediate zone where landforms of glacial erosion are displayed in imperfect or embryo form. Finally, the highest summits bear no landforms of glacial erosion.

The pattern is well displayed in the case of the Mt. Rea massif, including the summits of Mt. Rea and The Billboard (Figs. 2 and 5). The whaleback forms in the saddle to the south of the massif, as well as similar forms on the northeast and northwest spurs, occur up to an altitude of 410 m, and, in general, their orientation reflects ice flow diverging around the massif. At

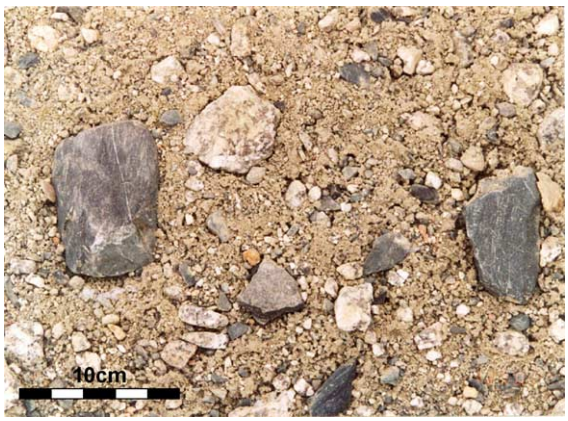

Fig. 7. Vertical close up of undisturbed till on the saddle between Mt. Rea and Mt. Dolber. The lighter-coloured clasts are granite. The darker clasts are metasediments, and the two larger examples are striated.

intermediate altitudes between 410 and 700 m, the landscape character is mixed. Scattered glacial striae, extensive smooth, rounded slabs and plucked joint surfaces point to the action of ice; yet, elsewhere, weathering pits, tor stumps and patches of reddish-brown weathering are similar to nonglacial features on the upper surfaces. The summit surface itself displays no evidence of glacial modification above 700 m. Here, upstanding tors of granite bedrock rise above a sea of large slabby or rounded boulders. The surfaces of boulders and tors are marked by sheeting often 10–20 cm apart and parallel to the overall summit surface (Fig. 8). There are weathering pits (up to 70×50 cm across and 30 cm deep), tafoni on some steeper flanks, and grus between boulders and in joints. The rock surfaces are weathered to a reddish-brown colour and are covered by a fragile surface layer of loose but not yet displaced crystals. The summit surface itself has slope angles not exceeding 26° but is dramatically truncated by near-vertical cliffs hundreds of metres high, overlooking surrounding glaciers. At all elevations, weathering pits filled with till and erratics lodged in cracks between tors and boulders show that ice has covered these upper surfaces (Fig. 9).

Similar altitudinal zonation occurs on other peaks. Streamlined glacial erosional forms are confined to the lower saddles of the Bailey and Asman ridges and Mt. Blades and to the lower slopes of Mt. Byrd. Further inland, at Mt. Darling, tors, weathering pits and grus also coexist with erratics at elevations above approximately 900 m. In all cases, landforms of glacial erosion become less obvious with increasing altitude and are gradually replaced with features characteristic of prolonged surface weathering.

5. Cosmogenic-nuclide exposure ages

In a previous paper (Stone et al., 2003b), we reported ^{10}Be exposure ages for glacial erratics in the study area. We reproduce a selection of these data in Fig. 10. In general, these show that all the summits in the field area were covered by overriding ice prior to 10,400 years B.P. and have been gradually uncovered during the Holocene. These data are important in the context of the present work because they tell us the duration of the present period of subaerial weathering. This period has been short, ranging from <2000 years near the present ice margin to 10,400 years close to the summit of the Mt. Rea massif.

We also found a second population of erratics whose total cosmic-ray exposure extends well back

Fig. 8. The surface of the tor on Mt. Rea showing the weathered surface and sheeting. Weathering pits occur on such surfaces, and grus lies in the surrounding joints. The weathered rock surfaces are reddish-brown in colour. (For interpretation of the references to colour in this figure legend, the reader is referred to the web version of this article.)

Fig. 9. An erratic lodged in a weathering pit on the surface of a tor on the Billboard.

beyond the most recent deglaciation (Tables 2A and 2B). Many of these 'old' erratics are faceted and striated and have lithologies that do not outcrop on any of the few nunataks exposed upstream of the field area, thus, we conclude that they were not initially exposed on mountain tops and then transported supraglacially to their present sites. Thus, the excess ^{10}Be and ^{26}Al in these samples must have

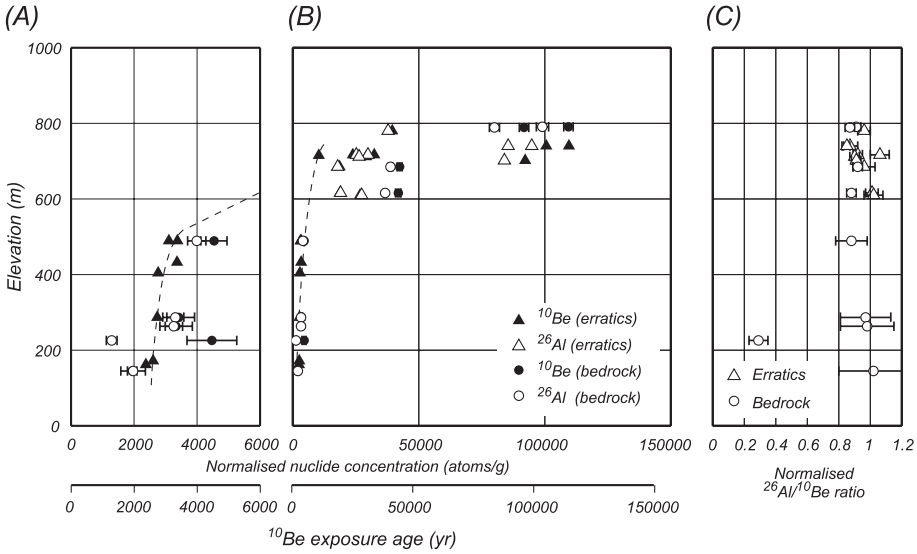

Fig. 10. Cosmogenic-nuclide concentrations in erratics and bedrock surfaces at various elevations on the Mt. Rea massif. (A) ^{10}Be and (B) ^{26}Al concentrations in erratics (see Stone et al., 2003b) and bedrock surfaces, all normalised to the local production rate for each sample and nuclide. For young samples, this quantity is approximately equivalent to the exposure age of the sample in years (lower scale). The dashed line shows the deglaciation history for Mt. Rea inferred from the youngest erratics. Only the axis limits differ between Panels (A) and (B). (C) normalised ^{26}Al/^{10}Be ratios. Normalised ratios less than 1 can only be achieved through extended cover of the samples by ice. Error bars in all figures show one standard error and include only analytical uncertainty. We do not include uncertainty in the production rates because this is a systematic error that would apply equally to all samples. Stone et al. (2003a) provide a more comprehensive error analysis for the exposure ages of the erratic samples.

Table 2A
Bedrock and Erratic Samples—Mt. Rea Massif: Site Details

Sample	Latitude (° S)	Longitude (° W)	Altitude (m asl)	Scaling (spallation)	Scaling (muons)	Thickness correction	Horizon correction
Erratics							
01-MBL-133-BBD	77.074	145.698	780	2.682	1.646	0.931	0.999
01-MBL-135-BBD	77.073	145.692	740	2.588	1.615	0.944	0.997
99-MBL-055-BBD	77.073	145.692	740	2.588	1.615	0.940	0.997
01-MBL-139-REA	77.078	145.584	717	2.534	1.597	0.956	0.994
01-MBL-140-REA	77.078	145.584	717	2.534	1.597	0.899	0.994
99-MBL-059-BBD	77.073	145.686	712	2.522	1.593	0.961	0.997
01-MBL-138-BBD	77.073	145.686	702	2.499	1.585	0.931	0.997
01-MBL-143-REA	77.077	145.587	685	2.460	1.572	0.956	0.998
01-MBL-146-REA	77.071	145.595	616	2.308	1.519	0.956	0.997
01-MBL-149-REA	77.071	145.595	610	2.295	1.515	0.948	0.997
Bedrock							
01-MBL-132-BBD	77.074	145.699	791	2.709	1.655	0.965	0.999
01-MBL-131-BBD	77.074	145.699	789	2.705	1.654	0.940	0.999
01-MBL-144-REA	77.077	145.587	685	2.459	1.572	0.948	0.997
01-MBL-148-REA	77.071	145.595	616	2.308	1.519	0.948	0.997
01-MBL-150-REA	77.068	145.575	489	2.046	1.425	0.948	0.998
01-MBL-154-REA	77.068	145.548	287	1.679	1.286	0.948	0.990
01-MBL-168-GAP	77.084	145.558	263	1.638	1.270	0.948	0.995
01-MBL-169-GAP	77.082	145.545	226	1.578	1.246	0.965	0.995
01-MBL-167-REA	77.061	145.568	145	1.451	1.194	0.952	0.967

been produced at their present locations in past interglacial exposure periods. The cumulative exposure time of these samples and their $^{26}Al/^{10}Be$ ratios provide some constraints on their history. $^{26}Al/^{10}Be$ ratios close to the production ratio of ~6 indicate continuous exposure. A significantly lower $^{26}Al/^{10}Be$ ratio implies one or more 'burial' periods (Bierman et al., 1999). In the Ford Ranges, 'burial' can only mean cover by the ice sheet, as there are no sedimentary deposits thick enough to shield samples from the cosmic ray flux. If we assume that these samples were exposed once and then covered by ice once, the ^{26}Al and ^{10}Be concentrations and their ratio provide a theoretical exposure age and duration of ice cover (Table 2B). Although these assumptions are oversimplified and the samples have almost certainly experienced much more complex exposure/ice cover histories, these theoretical 'exposure' and 'burial' ages are useful because they are minimum limits. A sample with an apparent exposure age of 100 kyr and an apparent burial age of 400 kyr records *at least* half a million years of exposure and ice cover since the last time the surface was eroded deeply enough to remove the existing nuclide inventory. For short periods of ice cover, we are limited by measurement error in the ^{26}Al and ^{10}Be concentrations: it is only possible to confidently distinguish continuously exposed surfaces from 'buried' ones after ~50–100 kyr of ice cover.

Half of the anomalously old erratics have $^{26}Al/^{10}Be$ ratios indistinguishable from the production ratio, indicating only short periods of ice cover since deposition. These samples record <40 kyr of cumulative cosmic ray exposure and, with one exception, their exposure times decrease with decreasing altitude. This pattern is most consistent with exposure at their present locations during one or more interstadial periods prior to the LGM, but within the last ~100 kyr. Five other erratics have $^{26}Al/^{10}Be$ ratios significantly below the production ratio, indicating ice cover for at least ~150–250 kyr (Table 2B; Fig. 10). All of these samples are above 700 m, but neither their apparent exposure age nor their $^{26}Al/^{10}Be$ ratio is correlated with elevation. In addition, their general appearance is indistinguishable from that of much younger erratics. We cannot derive a unique glacial history from these data, but they indicate that cumulative exposure totalling 100

Table 2B
Bedrock and Erratic Samples—Mt. Rea massif: isotopic details and exposure ages

Sample	^{10}Be production rate (atom/g/year)	[^{10}Be] (105 atom/g)	Apparent ^{10}Be Exposure age (kyr)	^{26}Al production rate (atom/g/year)	[^{26}Al] (105 atom/g)	Apparent ^{26}Al Exposure age (kyr)	^{26}Al/^{10}Be	Apparent burial age[a] (Myr)
Erratics								
01-MBL-133-BBD	12.5±0.7	4.93±0.11	39.7±2.5	76.4±4.6	28.9±1.11	38.6±2.8	5.86±0.26	n/a
01-MBL-135-BBD	12.2±0.7	13.36±0.3	112.2±7.3	74.5±4.5	70.68±3.59	99.6±8.3	5.29±0.29	0.25±0.15
99-MBL-055-BBD	12.2±0.7	12.27±0.15	103.2±6.4	74.2±4.5	63.41±1.66	89.3±6.2	5.17±0.15	0.28±0.14
01-MBL-139-REA	12.1±0.7	2.88±0.07	23.9±1.5	73.8±4.5	18.56±0.93	25.5±2	6.44±0.36	n/a
01-MBL-140-REA	11.4±0.7	3.68±0.07	32.5±2	69.4±4.2	20.69±0.67	30.2±2.1	5.62±0.21	n/a
99-MBL-059-BBD	12.1±0.7	3.53±0.08	29.3±1.9	73.9±4.5	19.4±0.49	26.6±1.8	5.50±0.19	0.23±0.14
01-MBL-138-BBD	11.7±0.7	10.78±0.18	94.4±5.9	71.1±4.3	59.7±1.64	87.6±6.1	5.54±0.18	0.19±0.12
01-MBL-143-REA	11.8±0.7	2.19±0.06	18.6±1.2	71.9±4.4	12.83±0.9	18±1.7	5.86±0.45	n/a
01-MBL-146-REA	11.1±0.7	2.07±0.05	18.8±1.2	67.4±4.1	12.75±0.43	19.1±1.3	6.16±0.25	n/a
01-MBL-149-REA	10.9±0.6	2.91±0.07	26.8±1.7	66.5±4	18.15±1.03	27.7±2.3	6.24±0.38	n/a
Bedrock								
01-MBL-132-BBD	13.1±0.8	14.33±0.24	112.2±7.1	79.9±4.8	79.12±1.96	104.2±7.2	5.52±0.17	0.19±0.12
01-MBL-131-BBD	12.7±0.8	11.65±0.24	93.3±6	77.7±4.7	62.16±1.56	83.3±5.7	5.34±0.17	0.24±0.13
01-MBL-144-REA	11.7±0.7	4.96±0.12	42.9±2.8	71.2±4.3	27.63±0.55	39.6±2.6	5.57±0.18	0.20±0.13
01-MBL-148-REA	11±0.7	4.6±0.12	42.4±2.8	66.8±4	24.47±0.4	37.3±2.4	5.32±0.16	0.26±0.15
01-MBL-150-REA	9.7±0.6	0.44±0.04	4.5±0.5	59.4±3.6	2.37±0.17	4±0.4	5.41±0.65	n/a
01-MBL-154-REA	7.9±0.5	0.27±0.04	3.4±0.6	48.4±2.9	1.6±0.13	3.3±0.3	6.01±1.05	n/a
01-MBL-168-GAP	7.8±0.5	0.26±0.04	3.3±0.6	47.5±2.9	1.55±0.13	3.3±0.3	6.02±1.08	n/a
01-MBL-169-GAP	7.6±0.5	0.34±0.06	4.5±0.8	46.5±2.8	0.6±0.08	1.3±0.2	1.75±0.39	2.35±0.5
01-MBL-167-REA	6.7±0.4	0.13±0.01	2±0.2	41.1±2.5	0.81±0.16	2±0.4	6.00±1.3	n/a

[a] Inferred from ^{26}Al/^{10}Be ratio relative to ratio expected for continuous exposure. Reported only for samples whose ^{26}Al/^{10}Be ratio was significantly (>95% confidence) below the production ratio of 6.1.

kyr or more results in limited chemical and physical degradation of granitic rocks in this part of Antarctica. This is an important conclusion for our interpretation of cosmogenic-nuclide concentrations in bedrock surfaces.

Tables 2A and 2B and Fig. 10 also show ^{26}Al and ^{10}Be concentrations in bedrock surfaces from the Mt. Rea massif. At elevations below 500 m, nuclide concentrations in both erratics and adjacent bedrock surfaces are low, and the nuclide concentration in bedrock can almost, but not completely, be accounted for by the present period of exposure. With one exception, the excess nuclide concentration in bedrock relative to nearby erratics increases with elevation. We attribute the low degree of inheritance in these low-elevation samples to subglacial erosion because of the geomorphic evidence described above and the idea that ice-free periods must necessarily be shorter at lower elevations. The observations that inherited nuclide concentrations increase with altitude and that all but one of the low-elevation bedrock samples have ^{26}Al/^{10}Be ratios within error of the production ratio argue that glacial erosion is the primary reason for low nuclide concentrations in bedrock near the base of the massif. If the last interglacial period was similar in length to the present one (~2000 years for the lowest sites), our data require subglacial erosion during the last glaciation to vary from zero above 500 m, ~40 cm at 260–290 m, to >40 cm at 145-m elevation (assuming that this lowest surface was previously exposed). One anomalous low-elevation sample (169 GAP) does, however, have both very low nuclide concentrations overall and a ^{26}Al/^{10}Be ratio significantly below the production ratio, suggesting a total exposure/ice cover history well in excess of 1 Myr.

At elevations above 500 m on Mt. Rea, all bedrock samples have high nuclide concentrations and ^{26}Al/^{10}Be ratios significantly below the production ratio (Table 2B; Figs. 10 and 11). Nuclide concentrations in bedrock always exceed those in nearby

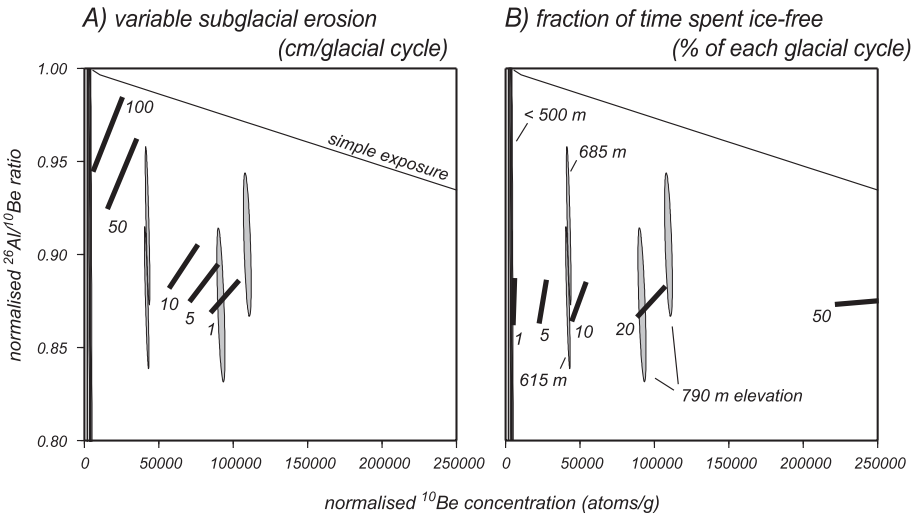

Fig. 11. ^{26}Al and ^{10}Be concentrations in bedrock from Mt. Rea compared with those predicted for various combinations of exposure time, duration of ice cover and subglacial erosion. The black bars show the expected nuclide concentrations in bedrock surfaces that have experienced four glacial–interglacial cycles, each of 100,000-year duration, and are now exposed during a fifth interglacial. The extent of the black bars reflects the possible range of nuclide concentrations expected at any time during the present interglacial (we show a range because the length of interglacials will likely be different for samples at different elevations). The grey shaded areas are 68% error ellipses for ^{26}Al and ^{10}Be measurements on bedrock samples from Mt. Rea. Note that the ^{26}Al/^{10}Be ratios of low-elevation, low-nuclide-concentration samples are very poorly constrained. In Panel (A), we assume that interglacial periods last for 20,000 years (20% of the total time) and vary the depth of subglacial erosion that occurs during glacials. The effect of increasing subglacial erosion is to lower the expected ^{10}Be concentration while increasing the expected ^{26}Al/^{10}Be ratio. In Panel (B), we assume that there is no subglacial erosion and vary the fraction of each glacial–interglacial cycle during which the surface is exposed. The effect of increasing the proportion of time exposed above the ice surface is to increase the expected ^{10}Be concentrations without appreciably changing the ^{26}Al/^{10}Be ratio. The high-elevation bedrock samples have similar ^{26}Al/^{10}Be ratios but a range of ^{10}Be concentrations and are therefore better explained by a scenario of negligible subglacial erosion but longer ice-free periods at higher elevations.

erratics. Nuclide concentrations increase with increasing elevation, but the ^{26}Al/^{10}Be ratio does not change measurably. Thus, the proportion of each sample's history during which it was exposed, rather than covered by ice, increases with elevation. The survival of these surfaces over at least 100 kyr of exposure and at least 150–250 kyr of ice cover requires low rates of both subglacial erosion and subaerial erosion during ice-free periods.

We cannot explicitly separate the effects of higher erosion rates at lower elevations and longer periods of exposure at higher elevations in producing the observed nuclide concentrations. Simple models of nuclide accumulation under various histories of exposure, ice cover and subglacial erosion suggest that the entire data set is best explained by a scenario of no subglacial erosion above 500 m, coupled with longer ice-free periods at higher elevations. The argument is outlined more fully in Fig. 11 and the accompanying caption. Assuming no subglacial erosion above 500 m, we can interpret nuclide concentrations in bedrock as a measure of the fraction of each glacial–interglacial cycle during which that surface is exposed (Cowdery et al., 2003; Fig. 11). Under this assumption, surfaces at 600–700 m have been exposed 10–15% of the time, and summit surfaces above 700 m have been exposed nearly half the time.

6. Discussion

The cosmogenic-nuclide data agree with the conclusions based on geomorphic mapping: Lower-elevation surfaces show evidence of modification by subglacial erosion, while higher-elevation surfaces show extensive evidence of subaerial weathering and no evidence of subglacial erosion. The data are best

explained by a scenario in which lower-elevation sites have experienced varying degrees of subglacial erosion, and higher-elevation sites have experienced both minimal erosion when covered by ice and longer exposure to periglacial conditions when free of ice. Thus, the altitudinal zonation of weathering zones reflects both englacial gradients in the effectiveness of subglacial erosion and the length of time that surfaces are ice-free.

6.1. Selective erosion beneath the ice sheet

The distribution of erratics up to and including the major summits of the area, and the lack of a distinct trimline marking the upper limit of glaciation imply, that the Sarnoff and Allegheny Mountains were once submerged by overriding ice. There is a consistent pattern of a decrease in the density of erratics with altitude, presumably due to the diversion of most overriding ice and any contained rock debris around obstructing massifs. There are many instances of this pattern in formerly glaciated midlatitudes of the northern hemisphere. For example, the Cairngorm Mountains in Scotland were covered by Pleistocene ice sheets and, although erratics occur high on the flanks of the massif, no erratics have been identified on the summits (Sugden, 1968).

Overriding ice flowed towards the WSW and SW. This is demonstrated by the concordance of ice-moulded landforms on the lower slopes and striations found at higher altitudes. At smaller scales, there is a topographic influence on the direction of flow reflecting divergence around upstanding massifs, as in the case of the Mt. Rea massif bounded by steep and high cliffs (Fig. 2). The consistency between different lines of evidence is noteworthy. For example on the saddle between Mts. Rea and Dolber, whalebacks, striations, larger grooves, crescentic chattermarks, the orientation of till streams and the imbricated alignment of large boulders trapped in the irregularities in the bedrock all point to ice sweeping south–westwards across the saddle towards Sulzberger Bay.

The pattern and distribution of the overriding glacial landforms is consistent with the presence of ice that was at the pressure melting point at its base, except over the higher summits, which were covered by cold-based ice. Warm-based ice is generally accepted to be necessary for effective glacial erosion because the presence of water facilitates basal sliding and erosion. The style of subglacial erosion indicated by the whalebacks, the high proportion of subangular stones, striated clasts and fine matrix in the till patches are all characteristic of glacial activity by warm-based ice. Although no unambiguous meltwater forms were identified, the presence of subrounded stones in the tills points to some subglacial meltwater transport. The cosmogenic-nuclide data from lower elevations likewise indicate that subglacial erosion did take place at these elevations; however, the amount of erosion during the last glaciation was small in most cases. Thus, the larger-scale ice-moulded landforms probably reflect subglacial erosion over many glacial–interglacial cycles, a conclusion agreeing with the findings of Stroeven et al. (2002) in Scandinavia.

On the other hand, the preservation of tors, boulder fields, weathering pits, grus and fragile weathered rock surfaces on the summits of Mts. Rea and Darling, combined with the absence of forms of glacial erosion, points to the protective role of ice in these locations. In the case of the Sarnoff and Allegheny Mountains, the presence of erratics among the tors and in weathering pits is convincing evidence that ice did cover the tors and, yet, was not able to modify them. High cosmogenic-nuclide concentrations in both erratics and bedrock surfaces demonstrate that both bedrock surfaces and boulders deposited during earlier glacial periods have survived multiple glaciations. This supports the geomorphic inference of minimal or no subglacial erosion at summit elevations. Such circumstances are believed to occur when the ice is cold based, and as a consequence, there is little meltwater and scope for sliding between ice and rock. Since many erratics are faceted and shaped by ice abrasion, they are likely to have originated in a zone of warm-based ice upstream of the mountains.

The pattern of warm-based ice at lower altitudes and cold-based ice at high altitudes and a transition between the two is a function of both ice thickness and topography. The thicker the ice, the warmer the basal ice will be (Robin, 1955). In addition, variations in velocity as the ice converges through saddles or diverges around massifs causes differential strain

heating and introduces an additional topographic relationship whereby upstanding hills tend to be cold based and surrounding lowlands warm based. This is well seen on the bed of the former Laurentide ice sheet (Sugden, 1978), in Scotland (Glasser, 1995) and Scandinavia (Kleman et al., 1999).

6.2. Weathering zones

The cosmogenic-nuclide data reinforce the conclusion that weathered surfaces at higher elevations must be ice-free for longer periods than those at lower elevations. The implication is that weathered summit landscapes are protected by cold-based ice during glacial periods and develop when they are free of ice during interglacials. At such latter times, they are exposed to chemical and physical attack under periglacial conditions.

6.3. Evidence of recent deglaciation

We can also use geomorphological data to evaluate the important question of whether the Holocene ice sheet thinning inferred from exposure ages of glacial erratics has continued to the present. The exposure ages reported in Stone et al. (2003b) suggest continued thinning toward the present, but their relationship to the actual level of the major glaciers is confused by the presence of ice slopes fed by local glaciers skirting many of the mountains. The geomorphological evidence concerns the fresh till covering on smooth, sloping rock surfaces within tens of metres of the ice edge on the northern side of the Mts. Rea–Dolber saddle. The preservation of unconsolidated material on smooth rock surfaces with slopes of up to 22° suggests that it cannot have been exposed to the elements for more than a matter of decades. Had it done so, it would have been removed from all but bedrock hollows, as occurs progressively upslope. We interpret the steady upslope reduction in the angle of till-covered slopes, as well as the concomitant winnowing of the till deposits, as evidence that ice retreat from these slopes has continued to the present.

6.4. Comparison with ice-sheet models

The evidence of former ice flow directions reflects overriding conditions when the grounding line was further offshore. The last time this happened in West Antarctica was during the Last Glacial Maximum (Stone et al., 2003b; Anderson, 1999), and thus, it is instructive to compare findings with models of the Antarctic Ice Sheet at its maximum. Fig. 12 shows two such reconstructions, assuming that the Antarctic Ice Sheet extended to the offshore continental shelf edge. The upper profile can be taken as the thickest possible ice cover during the LGM for two reasons. First, it is calculated assuming equilibrium with LGM climatic, isostatic and sea-level conditions, whereas it is unlikely that there was sufficient time for the West Antarctic Ice Sheet to build up to equilibrium thickness during an ice age cycle of 100,000 years. Second, the model does not include a "flow enhancement" factor commonly used in ice sheet models to fit observed ice-sheet thicknesses. Details of the model are in Hulton and Mineter (2000). The lower profile is based more on a fit with empirical constraints and is drawn from Denton and Hughes (2002).

A three-dimensional run of the thicker maximum model predicts ice flow to the north–west at about 320°, perpendicular to the main line of the offshore shelf edge. This contrasts with the field evidence of more westerly to south–westerly flow ranging from 220° to 293°, with a mean value around 263°. Probably, the contrast is best explained by a contrast in ice thickness. Whereas the model reconstructs the maximum possible ice thickness, the field evidence reflects a thinner ice sheet with ice flow from the Ford Ranges towards the depression of Sulzberger Bay, some 120 km inshore of the shelf edge (Fig. 4). Although it is not possible to calculate ice thicknesses, it is possible to use the comparison to suggest that the overriding ice in the Sarnoff and Allegheny Mountains was thinner than at any full maximum. Such a conclusion makes sense, since the field evidence points to topographic control on ice flow sufficient to divert most erratics around the highest summits. Perhaps, at the Last Glacial Maximum, the highest summits were covered by a few hundreds of metres of ice, and the ice flowed from the inland dome of the Ford Ranges to Sulzberger Bay.

Three-dimensional thermomechanical models of the Antarctic ice sheet at its maximum can also add insight into the pattern of the basal thermal regime. Although the Hulton model operates on a grid cell of 40 km^2 and, thus, can give only a rough approx-

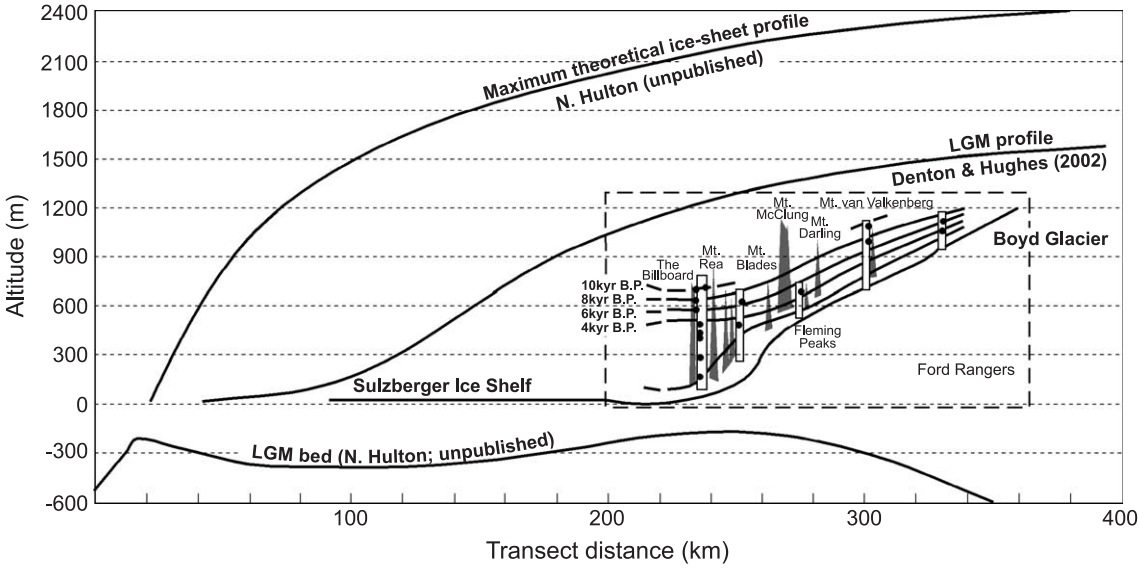

Fig. 12. Surface profiles for the Boyd Glacier compared with modelled ice-sheet profiles for the Last Glacial Maximum. The modelled profiles follow the Boyd Glacier from 152° W, 75° 15′ S to its mouth at 146° W, 76° 54′ S, then extend to the continental shelf edge at 152° W, 75° 15′ S. After the Supplementary notes in Stone et al. (2003b).

imation of conditions at the scale of the Sarnoff mountain topography, the full maximum model allows certain conclusions to be reached. The model predicts that cold-based ice covers broad upland areas of the Ford Ranges, but that warm-based ice occurs in the larger depressions. Such a broad pattern matches our evidence of just such a tendency throughout the Sarnoff and Allegheny Mountains. In the likely event that the ice sheet was thinner than modelled, then this topographically controlled tendency would be even stronger. What is striking about the field evidence is that it occurs at the scale of individual valleys, saddles and summits.

7. Conclusions

It is helpful to summarise the main conclusions with respect to Marie Byrd as follows:

- The juxtaposition of weathered upper surfaces and glacially moulded lower slopes in the Sarnoff and Allegheny mountains is primarily, but not exclusively, the result of contrasts in basal thermal regime beneath formerly overriding ice. Cosmogenic-nuclide analyses of erratics show that the ranges have been overridden on several occasions, most recently during the Last Glacial Maximum. Analyses of bedrock surfaces show that subglacial erosion occurred at lower elevations, probably to depths of tens of centimetres, but was insignificant at higher elevations. This rules out the hypothesis that the weathering contrast reflects a periglacial trimline marking out former nunataks. However, the weathering contrast is also a reflection of longer subaerial exposure times at higher elevations.
- The preservation of weathered surfaces, tors, grus and erratics beneath overriding ice is yet another example of the ability of glaciers to protect the surfaces over which they flow. The implication is that processes of erosion by cold-based ice, however, well based in theory and/or observation, play a limited role in landscape change, at least on longer time scales.
- Exposure ages exceeding 100,000 years on erratics that retain their glacial facets and fresh appearance imply low rates of periglacial weathering under interglacial conditions, at least on the upper surfaces. This supports the idea that the deeply weathered summit landscapes are the result of exposure during many successive interglacial

periods. However, the presence of cliffs associated with bergschrunds at the head of local glaciers and the presence of rockfall material in local ice moraines demonstrate effective denudation at lower altitudes.

- The direction of flow of overriding ice was towards a regional topographic low rather than to the outer shelf, implying that the LGM ice sheet was thinner than would have occurred had it achieved equilibrium maximum conditions.
- The pattern of glacial erosion and protection is the result of topographic control of ice thickness and velocity at the scale of individual valleys, saddles and summits. Streamlined whaleback forms occur within hundreds of metres of weathered tors. The amount of erosion inferred from cosmogenic-nuclide analyses of glacially modified surfaces also varies widely over short distances.
- As the ice sheet thinned during the last 10,400 years, the regional flow of overriding ice has given way to radial outflow by local ice masses centred on individual massifs. This has resulted in abrupt changes in ice flow direction in many situations.

Finally, there is the question of whether the findings in this part of Antarctica have a wider application, especially to the peripheries of former midlatitude ice sheets in the Northern Hemisphere. There are locations in Scandinavia, the UK, Greenland and North America where uplands with tors and other weathering forms survive in areas surrounded by lowlands with landforms of glacial erosion. A similar approach, combining geomorphology and cosmogenic isotope analysis, could establish whether when and for how long such landscapes have been inundated by ice.

Acknowledgements

This research was supported by the Office of Polar Programs of the National Science Foundation of the United States of America (grant numbers OPP-9909778 and OPP-9615282) and the Natural Environment Research Council of the United Kingdom. G. Balco was supported by a graduate fellowship from the Fannie and John Hertz Foundation. We thank Chuck Kurnik and Bjorn Jahns of UNAVCO for GPS support, and Marc Caffee and Bob Finkel of Lawrence Livermore Center for Accelerator Mass Spectrometry for their help with analyses. Kurt Krigbaum, Peter Apostle and Delina Carrasco assisted with sample preparation. Jon Harbor, Carolyn Eyles and Stewart Jamieson made many helpful comments.

References

Anderson, J.B., 1999. Antarctic Marine Geology. Cambridge University Press (289 p.).

Atkins, C.B., Barrett, P.J., Hicock, S.R., 2002. Cold glaciers erode and deposit: evidence from the Allan Hills, Antarctica. Geology 7, 659–662.

Ballantyne, C.K., 1990. The Late Quaternary glacial history of the Trotternish Escarpment, Isle of Skye, Scotland, and its implications for ice-sheet reconstruction. Proceedings of the Geologist's Association 101, 171–186.

Ballantyne, C.K., McCarroll, D., Nesje, A., Dahl, S.O., Stone, J.O., 1998. The last ice sheet in north-west Scotland: reconstruction and implications. Quaternary Science Reviews 17, 1149–1184.

Bierman, P.R., Marsella, K.A., Patterson, C., Davis, P.T., Caffee, M., 1999. Mid-Pleistocene cosmogenic minimum-age limits for pre-Wisconsinan glacial surfaces in southwestern Minnesota and southern Baffin Island, a multiple nuclide approach. Geomorphology 27, 25–39.

Briner, J.P., Miller, G.H., Davis, P.T., Bierman, P.R., Caffee, M., 2003. Last glacial maximum ice sheet dynamics in Arctic Canada inferred from young erratics perched on ancient tors. Quaternary Science Reviews 22, 437–444.

Boyer, S., Pheasant, D., 1974. Delimitation of weathering zones in the fiord area of eastern Baffin Island, Canada. Geological Society of America Bulletin 85, 805–810.

Cowdery, S., Stone, J.O., Finkel, R., 2003. Pliocene-Pleistocene Glacial History of Marie Byrd Land, West Antarctica, from Cosmogenic Nuclides in Bedrock Geological Society of America Annual Meeting, Seattle, Washington. Abstract 42-6.

Cuffey, K.M., Conway, H., Gades, A.M., Hallet, B., Lorrain, R., Severinghaus, J.P., Steig, E., Vaughn, B., White, J.C., 2000. Entrainment at cold glacier beds. Geology 28, 351–354.

Denton, G.H., Hughes, T.J., 2002. Reconstructing the Antarctic Ice Sheet at the last glacial maximum. Quaternary Science Reviews 21, 193–202.

Fabel, D., Stroeven, A.P., Harbor, J., Kleman, J., Elmore, D., Fink, D., 2002. Landscape preservation under Fennoscandian ice sheets determined from in situ produced ^{10}Be and ^{26}Al. Earth and Planetary Science Letters 201, 397–406.

Glasser, N.F., 1995. Modelling the effect of topography on ice sheet erosion, Scotland. Geografiska Annaler 77A, 67–82.

Hulton, N.R.J., Mineter, M.J., 2000. Modelling self organisation in ice streams. Annals of Glaciology 30, 127–136.

Kleman, J., Stroeven, A.P., 1997. Preglacial surface remnants and quaternary glacial regimes in northwestern Sweden. Geomorphology 19, 35–54.

Kleman, J., Hättesrand, C., Clarhäll, A., 1999. Zooming in on frozen bed patches: scale-dependent controls on Fennoscandian ice sheet basal thermal zonation. Annals of Glaciology 28, 189–194.

Linton, D.L., 1949. Unglaciated areas in Scandinavia and Great Britain. Irish Geography 2 (25–33), 77–79.

McCarroll, D., Ballantyne, C.K., Nesje, A., Dahl, S.-O., 1995. Nunataks of the last ice sheet in northwest Scotland. Boreas 24, 305–323.

Nesje, A., 1989. The geographical and altitudinal distribution of block fields in southern Norway and its significance to the Pleistocene ice sheets. Zeitschrift für Geomorphologie. Supplementband 72, 41–53.

Nesje, A., Sjerup, H.P., 1988. Late Weichselian/Devensian ice sheets in the North Sea and adjacent land areas. Boreas 17, 371–384.

Orombelli, G., Baroni, C., Denton, G.H., 1990. Late Cenozoic glacial history of the Terra Nova Bay region, Northern Victoria Land, Antarctica. Geografia Fisica e Dinamica Quaternaria 13, 139–163.

Reichelt, L., 1961. Über Schotterformen und Rundungsgradanalyse als Feldmethode. Petermanns Geographische Mitteilungen 105, 15–24.

Robin, G. de Q., 1955. Ice movement and temperature distribution in glaciers and ice sheets. Journal of Glaciology 2, 523–532.

Shreve, R.L., 1984. Glacier sliding at subfreezing temperatures. Journal of Glaciology 30, 341–347.

Stone, J.O., Todd, C., Balco, G., 2003a. Extraction of Al and Be from quartz for isotopic analysis. http://depts.washington.edu/cosmolab/chem.html.

Stone, J.O., Balco, G.A., Sugden, D.E., Caffee, M.C., Sass III, L.C., Cowdery, S.G., Siddoway, C., 2003b. Holocene deglaciation of Marie Byrd land, West Antarctica. Science 299, 99–102.

Stroeven, A.P., Fabel, D., Hättesrand, C., Harbor, J., 2002. A relict landscape in the centre of Fennoscandian glaciation: cosmogenic radionuclide evidence of tors preserved through multiple glacial cycles. Geomorphology 44, 145–154.

Sugden, D.E., 1968. The selectivity of glacial erosion in the Cairngorm Mountains, Scotland. Transactions of the Institute of British Geographers 45, 79–92.

Sugden, D.E., 1978. Glacial erosion by the Laurentide ice sheet. Journal of Glaciology 20, 367–391.

Sugden, D.E., Watts, S.H., 1977. Tors, felsenmeer and glaciation in the northern Cumberland Peninsula, Baffin Island. Canadian Journal of Earth Sciences 14, 2817–2823.